THE ASTROPHYSICAL JOURNAL, 437:L87–L90, 1994 December 20

COMMON LYMAN-ALPHA ABSORPTION TOWARD THE QUASAR PAIR Q1343+2640A, B: EVIDENCE FOR LARGE AND QUIESCENT CLOUDS[1]

NADINE DINSHAW,[2] CHRIS D. IMPEY,[2] CRAIG B. FOLTZ,[3] RAY J. WEYMANN,[4] AND FREDERIC H. CHAFFEE[3]

Received 1994 September 2; accepted 1994 October 5

ABSTRACT

We present observations of the Lyα forest of the close quasar pair Q1343+2640A ($z_{em} = 2.029$) and B ($z_{em} = 2.031$). We detect eight absorption lines of Lyα common to both spectra and not attributable to metal-line systems in the redshift range $1.7 < z < 2.1$ and four lines which are seen in one spectrum but not the other. At the 9".5 separation of the two quasars, this implies a firm lower limit on the characteristic size of the Lyα clouds of 40 h_{100}^{-1} kpc (where $h_{100} \equiv H_0/100$ km s^{-1} Mpc^{-1}, $q_0 = 0.5$) at a redshift $z \simeq 1.8$. The upper limit on the cloud size is much more uncertain owing to the small number of observed lines, but taking the observed fraction of common lines at face value in the context of a simple model, the absorbers are shown to have radii smaller than about 310 h_{100}^{-1} kpc. Significant velocity and equivalent width variations are seen with an rms velocity difference of $\sim$65 km s^{-1} between the common absorption lines along the two lines of sight.

Subject headings: quasars: absorption lines — quasars: general

1. INTRODUCTION

The majority of the absorption lines of Lyα seen in the spectra of high-redshift quasars are thought to arise in cosmologically distributed, intervening "clouds," the origin and physical nature of which remain controversial. Distinguishing between competing models for the absorbers requires some knowledge of the size of the Lyα clouds. Currently, the best limits on the cloud sizes, derived from observations along the two lines of sight to gravitationally lensed and projected pairs of quasars, lie anywhere in the range from 25 to 500 h_{100}^{-1} kpc (Smette et al. 1992; Shaver & Robertson 1983).

In this *Letter*, we present spectra of the Lyα forest of the quasar pair Q1343+2640A, B, which was discovered in a Canada-France-Hawaii Telescope (CFHT) survey for faint quasars by Crampton et al. (1988). The quasars have redshifts of 2.029 and 2.031 and are separated on the sky by 9".5, corresponding to a linear separation of $\sim$40 h_{100}^{-1} kpc for $q_0 = 0.5$. Despite the fact that the quasars are faint ($B \sim 20.2$), this pair is particularly well suited for this type of study since they sample the clouds on linear scales comparable to the expected characteristic cloud sizes predicted by several theoretical scenarios (Sargent et al. 1980; Ikeuchi & Ostriker 1986; Rees 1986; Bond, Szalay, & Silk 1988).

2. OBSERVATIONS AND REDUCTONS

Spectra of Q1343+2640A, B were obtained during the period from 1994 March 11 to June 2 UT with the Multiple Mirror Telescope, using the Blue Channel Spectrograph equipped with a highly optimized Loral 3072 × 1024 CCD. An 832 line mm^{-1} grating blazed at 3900 Å in second order was used, along with a 1" slit, yielding a spectral resolution of 1 Å FWHM (0.35 Å pixel^{-1}), over the wavelength range $\sim$3300–4100 Å. First-order light was blocked by a solid $CuSO_4$ filter. Total integration times of 68,400 s and 64,800 s were accumulated on A and B, respectively. Exposures of a He-Ar-Cu calibration lamp were taken before and after each object exposure. No flux calibration standard stars were observed.

The spectra were reduced with the IRAF software package using standard techniques. Uncertainties in the wavelengths were primarily due to asymmetries in the line profiles of the comparison arc lamp and amounted to no more than $\sigma \simeq 0.15$ Å. The resulting spectra of Q1343+2640A, B are shown in Figure 1.

The continuum was defined for each quasar using a cubic spline fit, and each pixel in the spectrum was subsequently searched for absorption using line-finding routines based on the algorithms employed in the *Hubble Space Telescope* (*HST*) Quasar Absorption Line Key Project (Schneider et al. 1993). Equivalent widths and line positions were determined by fitting single or, in the case of obvious blends, multiple Gaussian profiles to all the candidate absorption lines. A preliminary line list, useful for eliminating absorption features that were members of metal-line systems, was assembled from lines with observed equivalent widths, $W > 3.5\sigma_W$. We then culled a subset of these lines with $W > 5\sigma_W$ to form the more conservative list presented in Table 1. Two lines which fell below this threshold but which satisfied our definition of a common absorption system (described below) were retained in order to investigate the impact of excluding possible Lyα pairs on our determination of the cloud size because they did not meet the $5\sigma_W$ equivalent width limit. We show later that the equivalent widths of the common features between the two lines of sight exhibit significant scatter about a line with unity slope, so the equivalent width cutoff itself introduces uncertainty into the observed number of common lines. Ideally, it would be better to use the complete set of lines with rest equivalent widths above some fixed value. However, given the significant variations in the signal-to-noise ratio (S/N) levels across the spectra, so limiting the line list reduces the number of lines to an intolerably low level.

Line identifications were made using the set of standard quasar absorption lines given in Morton, York, & Jenkins (1988). Our identifications of metal-line systems agree well with

[1] Observations reported here were obtained at the Multiple Mirror Telescope Observatory, a facility operated jointly by the University of Arizona and the Smithsonian Institution.

[2] Steward Observatory, University of Arizona, Tucson, AZ 85721.
[3] Multiple Mirror Telescope Observatory, Tucson, AZ 85721.
[4] Carnegie Observatories, 813 Santa Barbara Street, Pasadena, CA 91101-1292.

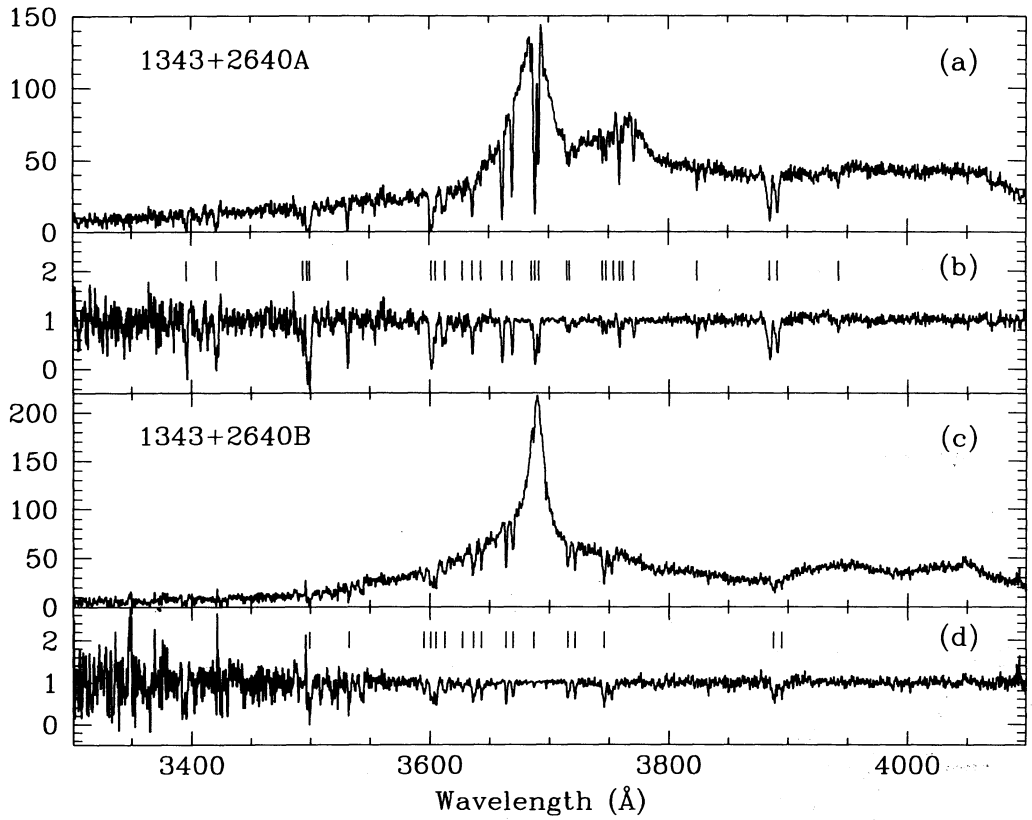

FIG. 1.—Spectra of Q1343+2640A, B. Panels (*a*) and (*c*) show the spectra in raw counts. In panels (*b*) and (*d*), the spectra have been divided by the continuum fits. Tick marks in (*b*) and (*d*) indicate absorption features with equivalent widths, $W > 5\sigma_W$. The wavelengths are vacuum and heliocentric.

TABLE 1

ABSORPTION LINES OF QUASAR PAIR Q1343+2640A, B

A No.	λ_{obs}(Å)	σ_λ	W_{obs}(Å)	σ_W	S/N	ID	z_{abs}	B No.	λ_{obs}(Å)	σ_λ	W_{obs}(Å)	σ_W	S/N	ID	z_{abs}	A–B Δv(km/s)
1	3395.98	0.19	1.83	0.31	5.8	Lyα	1.7935				< 1.95					
2	3421.19	0.19	2.96	0.36	8.2	Lyα	1.8142				< 2.50					
3	3494.02	0.13	1.29	0.21	6.1	Lyα	1.8742				< 1.42					
4	3497.58	0.10	2.02	0.34	6.0	Lyα	1.8771				< 1.35					
5	3499.77	0.13	2.76	0.38	7.4	Lyα	1.8789	1	3499.40	0.19	1.94	0.35	5.5	Lyα^2	1.8786	31 ± 20
6	3531.57	0.08	1.73	0.17	10.5	Lyα	1.9050	2	3532.31	0.20	1.28	0.22	5.9	Lyα	1.9057	-63 ± 18
			< 0.63					3	3595.07	0.21	0.62	0.12	5.1	Lyα	1.9573	
7	3601.73	0.09	3.42	0.20	16.7	Lyα	1.9628	4	3600.78	0.17	0.88	0.16	5.3	Lyα	1.9620	79 ± 16
8	3605.08	0.12	0.76	0.14	5.6	Lyα	1.9655	5	3605.28	0.09	1.21	0.11	11.0	Lyα	1.9657	-16 ± 12
9	3613.30	0.15	1.26	0.24	5.4	Lyα	1.9723	6	3612.52	0.25	0.86	0.13	6.4	Lyα	1.9716	64 ± 27
10	3627.86	0.14	0.40	0.09	4.4	Lyα	1.9843	7	3627.50	0.18	0.44	0.08	5.9	Lyα	1.9840	30 ± 19
11	3636.19	0.08	1.53	0.11	13.9	Lyα	1.9911	8	3636.60	0.11	1.42	0.10	13.5	Lyα	1.9914	34 ± 11
12	3643.14	0.14	0.31	0.07	4.1	Lyα	1.9968	9	3643.36	0.08	0.81	0.06	12.4	Lyα	1.9970	-18 ± 13
13	3661.10	0.03	1.95	0.06	35.5	Si III 1206	2.0345									
			< 0.24					10	3663.85	0.04	0.79	0.04	17.4	Ly$\alpha^{3,4}$	2.0138	
14	3669.48	0.03	1.23	0.04	30.8	Lyα	2.0185	11	3669.56	0.06	0.71	0.05	15.9	Lyα^3	2.0185	-6 ± 5
15	3685.36	0.05	0.25	0.02	10.0	Lyα	2.0316	12	3686.99	0.08	0.16	0.02	8.0	Lyα	2.0329	-132 ± 2
16	3688.54	0.01	2.29	0.03	76.5	Lyα^1	2.0342				< 0.11					
17	3691.58	0.01	1.25	0.03	50.0	Lyα^1	2.0367				< 0.11					
18	3715.07	0.11	0.35	0.06	5.3	C IV 1548	1.3996	13	3715.50	0.09	0.82	0.06	12.6	C IV 1548	1.3999	
19	3717.19	0.11	0.47	0.07	6.8	C IV 1548	1.4010									
								14	3721.36	0.07	0.65	0.06	11.8	C IV 1550	1.3997	
20	3744.88	0.06	0.36	0.04	8.0	C IV 1548	1.4189	15	3745.71	0.08	1.51	0.24	6.3	C IV 1548	1.4194	
21	3747.71	0.09	0.50	0.05	10.0	C IV 1548	1.4207									
22	3754.06	0.10	0.19	0.04	5.4	C IV 1550	1.4208									
23	3758.98	0.04	0.91	0.04	20.2	N V 1238	2.0343									
24	3761.92	0.09	0.27	0.04	6.9	N V 1238	2.0367									
25	3770.98	0.05	0.73	0.05	16.1	N V 1242	2.0343									
26	3824.03	0.06	0.43	0.06	7.8	Si II 1260	2.0339									
27	3884.94	0.08	2.73	0.13	20.3	C IV 1548	1.5093									
								16	3887.94	0.20	1.41	0.22	6.3	C IV 1548	1.5113	
28	3891.33	0.09	2.05	0.12	17.8	C IV 1550	1.5093									
								17	3894.65	0.23	0.72	0.15	5.0	C IV 1550	1.5114	
29	3942.39	0.19	0.43	0.09	5.1	Fe II 2600	0.5162									

NOTES.—Upper W_{obs} limits are for 5 σ significance level. For the sample of 5 σ lines, the line pairs A5-B1, A6-B2, A7-B4, A8-B5, A9-B6, A11-B8, A14-B11, and A15-B12 are coincidences and A2, A4, B9, and B10 are anticoincidences, according to the definitions outlined in the text. If we include the two 4 σ lines, then line pairs A10-B7 and A12-B9 are coincidences with B9 no longer being an anticoincidence. Superscripts denote the following: (1) member of metal-line absorption system; (2) probable blend with Si IV 1393 of C IV system $z = 1.5114$; (3) possible member of C IV doublet; and (4) probable blend with Si II 1526 of C IV system $z = 1.3998$.

Crotts et al. (1994), taking into account the higher resolution of our data which occasionally resolved close blends.

3. COMMON LYMAN-ALPHA ABSORPTION

Table 1 lists 14 Lyα forest lines in A and 12 in B with equivalent widths $>5\sigma_W$ from $z \simeq 1.79$ to the emission redshifts of the quasars. The distribution of velocity differences, Δv, of the absorbers between the two lines of sight was calculated from the fitted wavelengths of the features. For any given line, Δv was calculated only between the line itself and the "nearest neighbor" line in the spectrum of the other quasar, thereby restricting a given Lyα line to belong to at most one pair. The histogram of Δv calculated using all the detected Lyα forest lines in Table 1 shows a peak with FWZI of ~ 150 km s^{-1}, mean of -1 ± 17 km s^{-1} and median of 30 km s^{-1}, and no additional pairs out to velocity differences of ~ 2000 km s^{-1}. The estimated number of *random* Lyα pairs with $|\Delta v| < 150$ km s^{-1} is small, less than ~ 0.2, so we assume that the Lyα lines above the 5 σ equivalent width limit with a corresponding match within the velocity difference ± 150 km s^{-1} to be coincident to both spectra.

Under this criterion, of the 5 σ Lyα absorption lines in Table 1, eight are common. An ambiguity in the velocity matches arises in one case: Lyα line 12 in B could have been matched with either the lines 15 ($\Delta v = -132$ km s^{-1}) or 16 ($\Delta v = +126$ km s^{-1}) in A. It is possible that this is either a spurious match or reflects real clustering of Lyα forest lines on small scales. We decided to pair lines 12 (in B) and 15 (in A) since their equivalent widths are more closely matched. In addition to the eight common absorption lines, there are two "possible" cases where a match was found in velocity, but one component has an equivalent width less than 5 σ but more than 4 σ (lines 10 and 12 in A). Assuming identical clouds, a firm lower limit on the diameter of the absorbers equal to the angular-diameter distance between the two lines of sight may be established, independent of any assumptions about the variation of the cloud density with impact parameter; in this case, $D \sim 40\ h_{100}^{-1}$ kpc. We note that although we refer to "cloud size" in this *Letter*, we cannot distinguish between coherent entities and correlated but distinct structures, i.e., large ensembles of smaller clouds.

We chose to designate an absorption feature to be *not* in common to both spectra, or anticoincident, if the line is present in one spectrum at the 5 σ level and if a line of the strength would have been a 5 σ line in the other spectrum, but no corresponding 5 σ line is seen within the velocity difference ± 150 km s^{-1}. Four 5 σ Lyα lines, not identified with metal-line systems, met the above criteria.

The size of the Lyα clouds was estimated by means of Monte Carlo simulations. We assumed the simplest (admittedly unphysical) model wherein all clouds are identical, are spherical, and have constant column density. The simulations are very similar in detail to those reported by Smette et al. (1992) and result in the determination of the ratio, f, of the number of coincidences, N_C, to the number of coincidences plus anticoincidences, N_A, which when compared to the observed ratio gives the characteristic cloud size. Simulations were performed for cloud radii in the range $20 \leq R \leq 500$ kpc in steps of 20 kpc. At each R, 10,000 realizations were carried out, each consisting of randomly selected positions for $N_C + N_A$ clouds. The mean value of f and the range of f in which 95% of the realizations fell were calculated and are plotted in Figure 2.

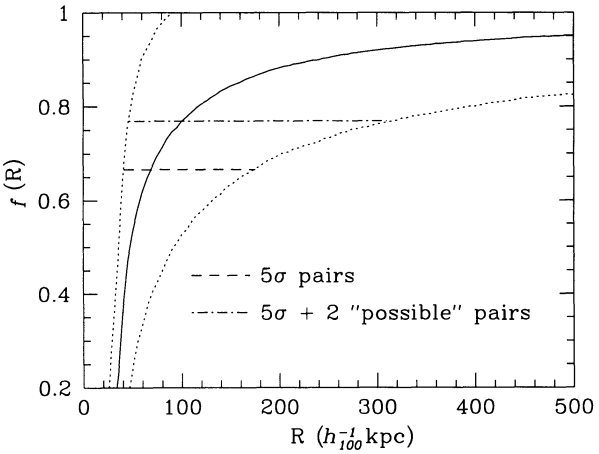

FIG. 2.—Fraction of common absorbers as a function of cloud radius. The solid curve gives the ratio f of the number of coincidences to the sum of the coincidences and anticoincidences as a function of cloud radius for the two samples described in the text. The dotted curves indicate the lower and upper limits on the radius of the absorbers at the 95% confidence level. A cosmological model with $H_0 = 100$ km s^{-1} Mpc and $q_0 = 0.5$ was assumed.

Two samples were considered: In the first case, we consider only pairs where both components have equivalent widths >5 σ; specifically, $N_C = 8$ and $N_A = 4$, giving $f = 0.67$. The characteristic radius R from Figure 2 is 70 h_{100}^{-1} kpc with lower and upper limits of $41 < R < 175\ h_{100}^{-1}$ kpc. In the second case we included the two "possible" common absorption features giving a total number of lines of 13 with $N_C = 10$ and $N_A = 3$, or $f = 0.77$. The characteristic cloud radius is large since f increases: $R \simeq 100\ h_{100}^{-1}$ kpc, with lower and upper limits of $46 < R < 310\ h_{100}^{-1}$ kpc. (Note that for $q_0 = 0$, these numbers increase by $\sim 50\%$.)

Putting aside the simple-minded assumptions of the simulation (i.e., spherical clouds, no evolution in cloud size, hard-edged clouds), the significance of the upper limits on the cloud size given above is accurate only if we know the fraction of coincident lines exactly. In fact, there is an intrinsic uncertainty in our determination of f arising from the small number of absorbers detected in the redshift window sampled by our observations. For example, if only one of our coincident pairs was in fact an anticoincidence (i.e., $N_C = 7$ and $N_A = 6$), f would drop to 0.54 with an attendant upper limit of about 110 h_{100}^{-1} kpc. Conversely, if two of the lines we call anticoincident were in fact coincident (i.e, $N_C = 9$ and $N_A = 2$), f would rise to 0.82 and the upper limit to about 500 h_{100}^{-1} kpc. Therefore, an error of ± 1 pair results in an uncertainty of almost a factor of 5 in the inferred upper limit. For $f > 0.95$, the upper limit on the cloud radius is indeterminate.

Differences in equivalent widths and wavelengths of the common absorption features probe the column density and bulk motion along lines of sight separated by scales of 40 kpc. Existing data from Foltz et al. (1984) and Smette et al. (1992) indicate that the clouds are remarkably homogeneous and quiescent on scales of a few kiloparsecs. Our results suggest that we are sampling the clouds on spatial scales for which these properties do change. The rest equivalent widths of the common features along each sight line are plotted against each other in Figure 3. A χ^2 test shows that the distribution is inconsistent with a line with unity slope at more than a 99.9% significance level (reduced $\chi^2 = 36$), implying that on scales of

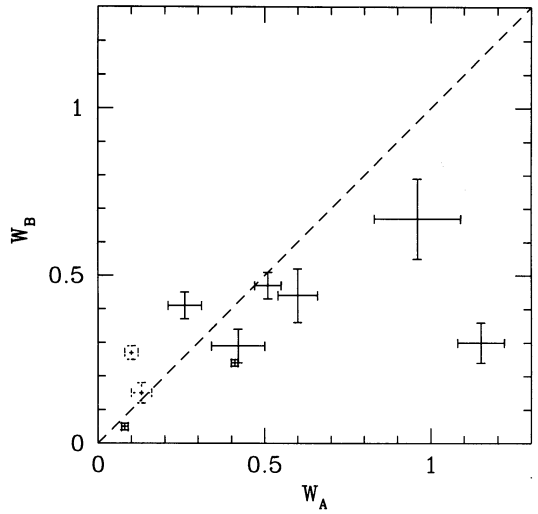

FIG. 3.—Correlation between the rest equivalent widths of the common lines in Q1343+2640A, B. The dotted error bars represent the two "possible" cases of common absorption. The dashed line has unit slope.

$\sim$40 kpc the column densities through the clouds do not correlate as well as they do when sampled on the 1–2 kpc scale of the Smette et al. (1992) study. The rms velocity difference is 65 km s^{-1} for the eight coincident lines and 60 km s^{-1} when the two possible coincidences are included. The 1 σ uncertainty in the wavelength calibration is about 13 km s^{-1}, and the typical uncertainty in the Gaussian fits is $\sim$20 km s^{-1}, which when combined in quadrature give a total uncertainty of $\sim$24 km s^{-1}, so the rms velocity differences deviate from zero at the 2.7 σ and 2.5 σ levels, respectively. The significance of this result is not overwhelming, but we interpret it as an indication that we are seing real, albeit small, differences in the projected radial velocities of the clouds on scales of $\simeq 40\, h_{100}^{-1}$ kpc.

4. DISCUSSION

The observations presented here give a direct and model-independent lower limit on the absorber diameter of $\sim 40\, h_{100}^{-1}$ kpc, suggesting further that they may be very large, with sizes up to 100 kpc or more. We also detect differences in the column density and radial velocity of the absorbing gas on these scales. Every leading model has difficulty explaining Lyα clouds that are as large and quiescent as these observations imply.

The characteristic radius of 70–80 h_{100}^{-1} kpc is substantially larger than that predicted by two popular models: clouds confined by a hot intergalactic medium (Sargent et al. 1980) and gas confined by minihalos of cold dark matter (Rees 1986). The characteristic velocity difference of 60–65 km s^{-1} is also a severe constraint. For example, clouds in the disks or virialized halos of normal galaxies would produce velocity dispersions of 200–300 km s^{-1} (Mo & Morris 1994). Recent N-body simulations, which treat baryons and dark matter as gravitationally coupled fluids, have looked at the dynamics of galaxies or baryonic lumps that will become galaxies (Evrard, Summers, & Davis 1994). At $z \sim 2$ and on scales of 50–500 kpc, the one-dimensional pairwise peculiar velocity dispersion is 200–400 km s^{-1}.

Recently, Morris & van den Bergh (1994) have speculated that a significant fraction of Lyα absorbers might be associated with tidal debris in small groups of galaxies. Even in a low velocity dispersion environment, a conservative upper limit of 150 km s^{-1} on the velocity difference between separate lines of sight is difficult to accommodate. The archetype for this environment, the Local Group, has a line-of-sight velocity dispersion of about 150 km s^{-1} (Zaritzsky 1994). Double galaxies, including those with tidal tails and distortions and common halos, have characteristic radial velocity differences of 200–300 km s^{-1} (Tifft 1985). However, it is not clear whether the tidally stripped material will reflect the velocity differences of the parent galaxies. If the absorbers have simple geometries near the upper end of the allowed range, $\sim$500 kpc, then the gas must be in a state that approximates pure Hubble flow.

This research was supported by the National Science Foundation under grant AST 93-20715, for which we are very grateful. We acknowledge Mike Lesser, Dave Ouellette, Gary Schmidt, and the Steward Observatory CCD Group, whose assiduous work, supported in part by NSF grant AST 91-21801, resulted in the CCD detector which made these observations possible. We thank Tom Aldcroft and Jill Bechtold for making their spectral analysis software available to us.

REFERENCES

Bond, J. R., Szalay, A. S., & Silk, J. 1988, ApJ, 324, 627
Crampton, D., Cowley, A. P., Hickson, P., Kindl, E., Wagner, R. W., Tyson, J. A., & Gullixson, C. 1988, ApJ, 330, 184
Crotts, A. P. S., Bechtold, J., Fang, Y., & Duncan, R. C. 1994, ApJ, 437, L79
Evrard, A. E., Summers, F. J., & Davis, M. 1994, ApJ, 421, 11
Foltz, C. B., Weymann, R. J., Röser, H.-J., & Chaffee, F. H. 1984, ApJ, 281, L1
Ikeuchi, S., & Ostriker, J. P. 1986, ApJ, 301, 522
Mo, H. J., & Morris, S. L. 1994, MNRAS, 269, 52
Morris, S. L., & van den Bergh, S. 1994, ApJ, 427, 696
Morton, D. C., York, D. G., & Jenkins, E. B. 1988, ApJS, 68, 449
Rees, M. J. 1986, MNRAS, 218, 25
Sargent, W. L. W., Young, P., Boksenberg, M., & Tytler, D. 1980, ApJS, 42, 41
Schneider, D. P., et al. 1993, ApJS, 87, 45
Shaver, P. A., & Robertson, J. G. 1983, ApJ, 268, L57
Smette, A., Surdej, J., Shaver, P. A., Foltz, C. B., Chaffee, F. H., Weymann, R. J., Williams, R. E., & Magain, P. 1992, ApJ, 389, 39
Tifft, W. G. 1985, ApJ, 288, 65
Zaritsky, D. 1994, The Local Group: Comparative and Global Properties, 3d ESO/CTIO Workshop, in press